NE-CAT Communications

A Biannual Newsletter of the Northeastern Collaborative Access Team Summer 2014

Message from the Director

Steve Ealick

Were you at Quo Vadis Structural Biology 2014? While I was unable to attend the computing school, I heard it was very well attended and a great success. Special thanks go to David Neau, Jon Schuermann, and Piotr Sliz for organizing the computing school.

The first six months of 2014 has brought some exciting new hardware to NE-CAT. The long awaited large capacity sample automounter is finally here. This automounter is an NE-CAT creation from start to finish. The automounter was designed by Malcolm Capel based on our existing ALS-style automounters. The majority of components were machined by Ed Lynch. Finally, the control software was written by Jim Withrow. I am very enthused about the final machine and you can read more about it later in this newsletter.

If you would like to try the new sample automounter, check out our available beamtime at our website: http://necat.chem.cornell.edu.

Beamline Developments

1. Quo Vadis Structural Biology 2014?

From June 5 to June 7, NE-CAT joined with SBGrid to host a computing school in Boston on data processing in crystallography, structure determination with Phenix and structural modelling. The computing school was attended by over 150 people. Special thanks go to Michelle Ottaviano for arranging all the logistics associated with the school in Boston.

On Thursday, the computing school kicked off with a session that emphasized data and errors therein (Fig. 1). Jim Pflugrath and Zbyszek Otwinowski covered the techniques and errors of indexing, integration, scaling, and merging, followed by a very detailed talk from Kay Diederichs in which he shed some light on the various

Fig 1. Quo Vadis attendees in the Armenise Amphitheater on the Harvard University Longwood Campus. Jon Schuermann chairs the first session of the computing school.

statistics describing the errors of data and models. This was followed by a spirited discussion of the all-important Table 1, and then Piotr Sliz closed out the session with a detailing of SBGrid's contributions to macromolecular crystallography.

The Thursday afternoon session was a how-to on processing difficult data with several different programs. Phil Evans presented MOSFLM. Zbyszek Otwinowski covered the procedure in HKL-2000. Kay Diederichs presented XDS and Matt Benning, the twinned data specialist, covered using RLATT.

The Friday morning session was a great tutorial in how to squeeze the most from data collection time using current methodologies. Jon Schuermann discussed many tools available at NE-CAT, with a special emphasis on micro-crystallography. Raj Rajashankar described the method of collecting and combining many low-dose data sets called dose-slice data collection and was very convincing when he presented a series of tests of the method against more traditional high-dose data collection. Clemens Schulze-Briese highlighted the benefits of using the new Pilatus detectors, and David Neau gave an enlightening talk on what to do (and what not to do) to make the most of remote data collection time.

The Friday afternoon session comprised of two talks by Nick Sauter in which he described new methods for data analysis in the nascent DIALS package for MX data and the software that has been developed for handling XFEL data, cctbx.xfel. Frank Murphy covered the capabilities of the NE-CAT produced automated MX data analysis suite RAPD, and Dominika Borek gave much good advice on handling recalcitrant data with HKL-2000.

On Saturday morning, the winners from the poster session (Kevin Wang, Kotaro Kelley and Kevin Knockenhauer, Xiaofei Jia, Brian Bae, and Zahra Assur) each gave lightning fast talks on their research, making for a great start to the day. The Phenix team (Tom Terwilliger, Paul Adams, and Nat Echols) then gave a series of presentations that were both a tutorial on how to use Phenix and an update on new features in the software suite. Tom's new methods for weak SAD solutions were especially enticing.

Videos of the lectures from the computing school are available on the SBGrid YouTube Channel (https://www.youtube.com/user/SBGridTV).

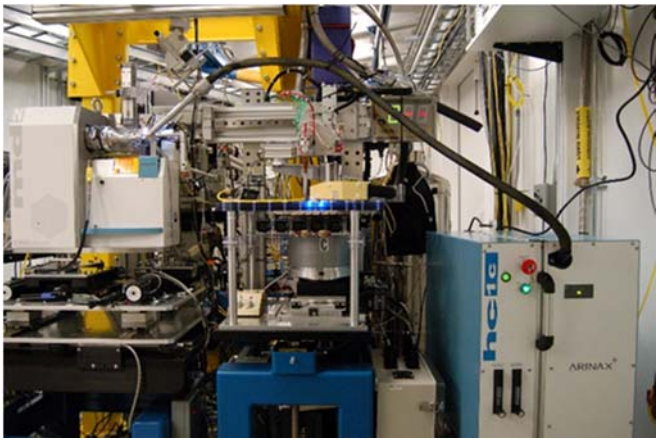

Fig. 2 Placement of the HC1 on 24-ID-E. The hose delivering the humid air is installed in place of the cryostream.

2. HC1, Crystal Humidity Controller

Described in the Winter 2013 newsletter (http://necat.chem.cornell.edu/newsletters/2013-winter.pdf), the HC1 was commissioned and calibration-tested by staff during the 2014-1 run with saturated salt solutions of a known relative humidity (RH). For example, saturated NaCl has a RH of ~75% at room temperature. If the RH of the HC1 is set below 75%, crystals of NaCl appear. Similarly, if the RH is set above 75%, these crystals dissolve in a repeatable manner.In addition, as the HC1 performed as expected with known protein crystals whose diffraction improved upon application of dehydration, select users were also invited to test the HC1 during the 2014-1 run cycle.

Currently, the HC1 can be installed on 24-ID-E in place of the cryostream (Fig. 2) and is available on an on-demand basis. Starting with the 2014-2 run cycle, the HC1 is available by request only during any scheduled beamtime. For users with known dehydration conditions, crystals could be dehydrated on Tuesdays

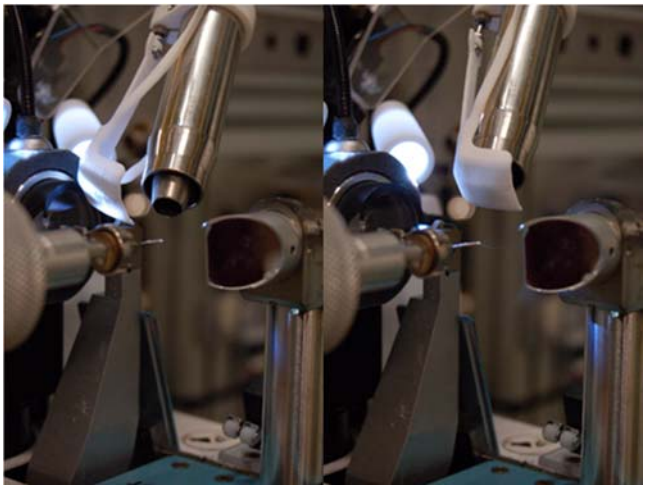

Fig. 3 Cryo-Shutter installed on the cryostream. The left image shows the shutter in the open position, where cryogenic gas flow is unimpeded. The right image shows the shutter in the closed position. The backlight remains up during the annealing process so that melting of the sample can be observed in real time.

when storage ring machine studies are in progress and stored for later data collection.

3. Remote Crystal Annealing Device

In the spring of 2014, NE-CAT also installed a new device for users who wish to anneal their crystals. Known as the 'Cryo-Shutter', the device cuts off the cryogenic gas stream on the sample (Fig. 3). While annealing can be carried out by manually blocking the cryostream (e.g. credit card, user ID badge), this device provides the convenience of doing the same remotely, without entering the hutch.

Annealing should only be performed on fresh crystals that have not been irradiated. Due to the intensity of the beam at the APS, exposure of cryogenically frozen crystals to X-rays results in the creation of hydrogen. When crystals are defrosted, the hydrogen is explosively released as gas, resulting in bubbles in the cryosolution, or in more extreme cases, utter decimation of the crystal. Currently, the minimum time recommended to fully melt a frozen sample is 8 seconds. However, users have the freedom to adjust the time and optimize it for their sample.

For local users, the cryo-shutter controls can be accessed through the sample changing or robot menu on the sample centering tab of the Auxiliary script. Implementation of commands to control the cryo-shutter during remote data collection is in progress.

4. Large Capacity Sample Automounter

For the last six months, NE-CAT has been constructing and programming a new sample automounter. This automounter has a high capacity dewar that can hold 14 ALS-style pucks for a total of 224 samples. The original design of the high capacity sample automounter was described in detail in the Summer 2013 newsletter (http://necat.chem.cornell.edu/newsletters/2013-summer.pdf).

At the end of May 2014, the new automounter was installed on 24-ID-C (Fig. 4), commissioned and made available to users for the 2014-2 run. Now fully built, the automounter comes with a new fan design for preventing ice formation on top and high intensity LED ring lights for illumination and improved sample visibility. The large capacity sample automounter has been tested on 24-ID-C during the summer and construction of a second automounter for 24-ID-E is in progress. It will incorporate changes that have been suggested by you, our users.

5. 24-ID-C Beamline Crosses 1000 PDB Deposits

As of July 2014, more than 1000 PDB entries are based on data collected at NE-CAT's 24-ID-C beamline. At the Advanced Photon Source (APS), there are currently 21 operational beamlines dedicated to macromolecular crystallography. Out of 21 beamlines, only 5 have more than 1000 depositions in the Protein Data Bank (PDB). The high number of PDB deposits indicates that 24-ID-C is an extremely successful beamline, allowing our users to collect high

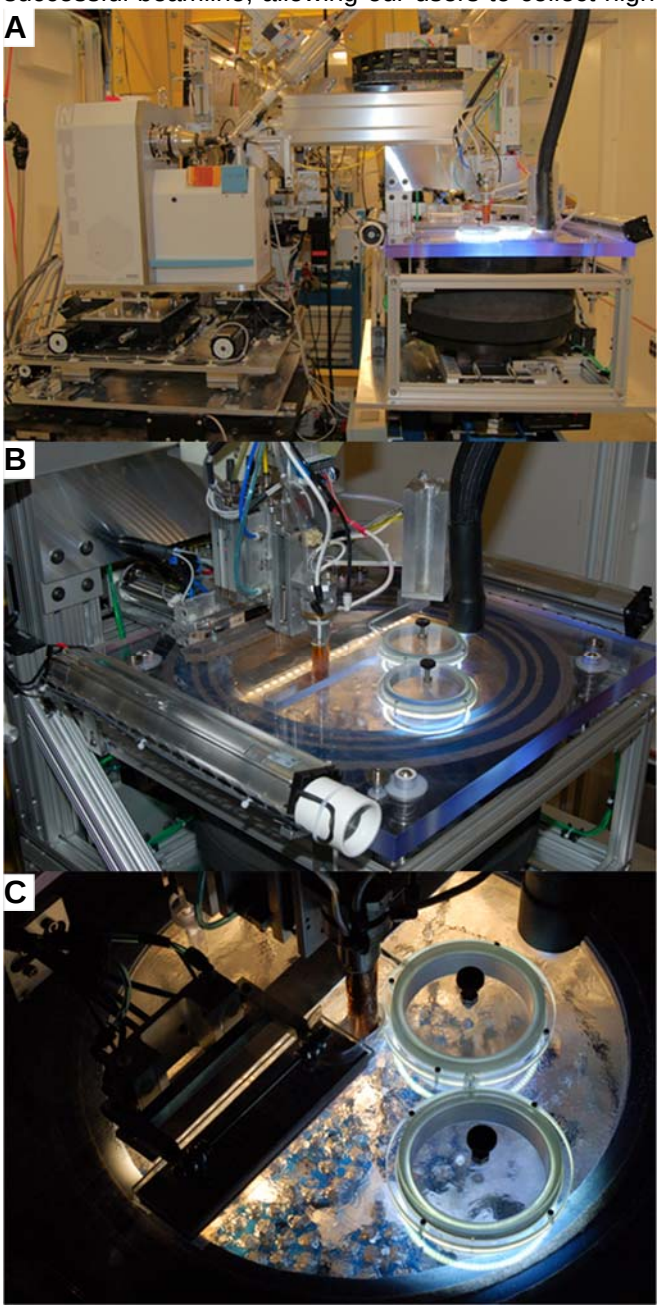

Fig. 4 A) Large Capacity Sample Automounter installed on 24-ID-C at the end of May 2014. B) The new slot mechanism for sample removal. In this photo, the gripper has moved from its position in the middle of the dewar and is preparing to mount a sample. C) Closeup of the 14 puck positions inside the dewar. Only 7 positions are filled in this photo.

quality data and solve many structures. NE-CAT's tunable beamline contributes 7% of the total deposited structures attributed to the APS and 1.4% of the total deposited structures from synchrotrons in the world. 24-ID-E, the second operational beam line of NE-CAT has already exceeded 500 PDB depositions.

Research Highlights

How lipophilic aromatic compounds are made in membranes

Weikai Li, Assistant Professor of Biochemistry and Molecular Biophysics, Washington University, St. Louis, MO.

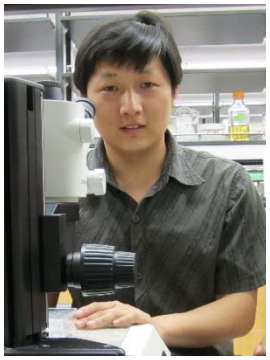

Wei Cheng, Postdoctoral Associate

Isoprenoid quinones are abundant in almost all living organisms and have the ideal chemical property to serve as the electron carrier in biological membranes. The quinone ring allows reversible redox reaction and the isoprenoid side chain provides the membrane solubility. A group of intramembrane enzymes, the UbiA superfamily of aromatic prenyltransferases, synthesize lipophilic quinones by joining a polar quinone head to a hydrophobic isoprenoid tail.

These UbiA superfamily enzymes produce a large variety of quinones as well as other lipophilic aromatic compounds including ubiquinones, menaquinones, plastoquinones, hemes, chlorophylls, vitamin E, and bacterial cell-wall lipids. Most of these lipophilic aromatic compounds serve as electron and proton carriers for cellular respiration and photosynthesis and as antioxidants to reduce cell damage. Mutations in eukaryotic superfamily members have been linked to cardiovascular degeneration, Parkinson's and other neurodegenerative diseases, and urologic cancers. Although the UbiA superfamily enzymes are fundamentally important to life, their catalytic mechanisms are largely unknown due to the lack of structural knowledge.

The archetypal UbiA enzyme catalyzes the condensation of isoprenylpyrophosphate (IPP) with the aromatic p-hydroxybenzoate (PHB). UbiA cleaves the pyrophosphate from the IPP substrate to generate a carbocation intermediate at the end of the isoprenyl chain, which reacts at the meta-position of the aromatic PHB substrate to form a C-C bond (Fig. 5A). Although the prenylation of PHB is regiospecific, UbiA promiscuously recognizes IPPs of various chain lengths to generate the ubiquinones $CoQ_{6\text{-}10}$ in different species.

The study (Cheng, W., and Li, W. (2014) Structural insights into ubiquinone biosynthesis in membranes, *Science 343*, 878-881.), conducted by researchers from Weikai Li's group at Washington University, investigated how this prenylation reaction is catalyzed inside the membrane. Using data collected at the APS 24-ID-C and -E, the researchers solved the crystal structures of an archaeal UbiA homolog in its apo and substrate-bound states. The structures reveal nine transmembrane helices and an extra-membrane cap domain that surround a large central cavity containing the active site (Fig. 5B). Two Asp-rich motifs in UbiA are likely to engage IPP through Mg-dependent interactions. To facilitate the catalysis inside membranes, UbiA has evolved an unusual active site that opens laterally to the lipid bilayer. During the condensation reaction, these long isoprenyl chains may extend through the lateral portal and directly contact lipid molecules (Fig. 5C). Thus, the lateral portal can facilitate the binding of long-chain IPP substrates and the prenylated products can be directly released into membranes through this portal. Without a defined chamber to restrict the chain length, UbiA can promiscuously recognize a variety of long-chain IPP substrates and generate the precursors of coenzyme Q of various lengths in different species. This is an interesting strategy that intramembrane enzymes can use to catalyze reactions in lipid bilayers.

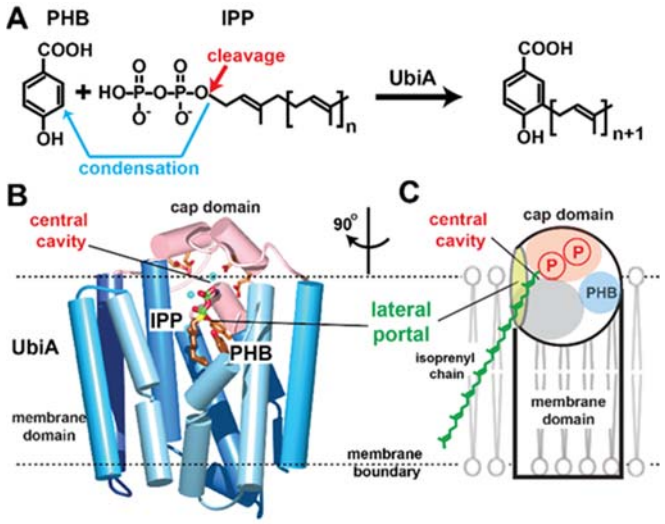

Fig. 5 A) The prenyltransferase activity of UbiA. This intramembrane enzyme cleaves off the pyrophosphate group from the IPP substrate and fuses the isoprenyl chain to the aromatic PHB substrate. B) Structure of an archaeal UbiA in complex with substrates. The cap domain is shown in pink and the transmembrane helices are shown in different blue colors. C) Cartoon representation of the structure. A unique lateral portal (green circle) opens to the lipid membrane and facilitates the binding and releasing of the isoprenyl chain. The large central cavity contains a polar pocket (pink) for pyrophosphate binding, a hydrophobic wall (grey) for the binding of isoprenyl chains, and a small basic pocket (blue) for PHB binding.

The UbiA structures reveal a catalytic mechanism that is generally applicable to all superfamily members catalyzing the synthesis of lipid-soluble aromatics, which are among the most important compounds found in biological membranes. These first structures of a UbiA-type enzyme provide a framework for future studies to understand other important superfamily members, and to design chemoenzymatic synthesis of new aromatic compounds with antiviral and anticancer activities. Moreover, the crystal structures provide a mechanistic understanding of disease-related mutations in eukaryotic superfamily members.

Staff Activities

Presentations

Raj Rajashankar, "Better Data, Not Crystals: Recent Advances in Synchrotron MX Data Collection," Molecular Biophysics Unit, Indian Institute of Science, Bangalore, India, February 20, 2014.

Kay Perry, "Automated Merging of Multiple Partial Datasets," 2014 Annual Meeting of the American Crystallographic Association, Albuquerque, New Mexico, May 24-28, 2014.

Jon Schuermann, "Optimizing Data Collection with Micro-Diffraction Tools," Quo Vadis Structural Biology 2014? SBGrid/NE-CAT Computing School, Harvard Medical School, Boston, Massachusetts, June 5-7, 2014.

Kanagalaghatta Rajashankar, "Dose-sliced Data Collection," Quo Vadis Structural Biology 2014? SBGrid/NE-CAT Computing School, Harvard Medical School, Boston, Massachusetts, June 5-7, 2014.

David Neau, "Getting the Most from Remote Data Collection," Quo Vadis Structural Biology 2014? SBGrid/NE-CAT Computing School, Harvard Medical School, Boston, Massachusetts, June 5-7, 2014.

Frank Murphy, "RAPD," Quo Vadis Structural Biology 2014? SBGrid/NE-CAT Computing School, Harvard Medical School, Boston, Massachusetts, June 5-7, 2014.

Surajit Banerjee, "NE-CAT: Crystallography Beamlines for Challenging Structural Biology Research" Vanderbilt Institute of Chemical Biology, Vanderbilt University, Nashville, Tennessee, August 1, 2014.

Session Chair

Jon Schuermann, "Introduction to Data Processing," Quo Vadis Structural Biology 2014? SBGrid/NE-CAT Computing School, Harvard Medical School, Boston, Massachusetts, June 5-7, 2014.

Publications

Zeqiraj, E., Tang, X., Hunter, R. W., Garcia-Rocha, M., Judd, A., Deak, M., von Wilamowitz-Moellendorff, A., **Kurinov, I.**, Guinovart, J. J., Tyers, M., Sakamoto, K., and Sicheri, F. (2014) Structural basis for the recruitment of glycogen synthase by glycogenin, *Proc. Nat. Acad. Sci. U.S.A. 111*, E2831-E2840.

Lee, K., Zhong, X., Gu, S., Kruel, A. M., Dorner, M. B., **Perry, K.**, Rummel, A., Dong, M., and Jin, R. (2014) Molecular basis for disruption of E-cadherin adhesion by botulinum neurotoxin A complex, *Science 344*, 1405-1410.

Bhattacharya, S., Lou, X., Hwang, P., **Rajashankar, K. R.**, Wang, X., Gustafsson, J. A., Fletterick, R. J.,

Jacobson, R. H., and Webb, P. (2014) Structural and functional insight into TAF1-TAF7, a subcomplex of transcription factor II D, *Proc. Nat. Acad. Sci. U.S.A.* [Epub ahead of print].

Bolla, J. R., Su, C. C., Do, S. V., Radhakrishnan, A., Kumar, N., Long, F., Chou, T. H., Delmar, J. A., Lei, H. T., **Rajashankar, K. R.**, Shafer, W. M., and Yu, E. W. (2014) Crystal Structure of the *Neisseria gonorrhoeae* MtrD Inner Membrane Multidrug Efflux Pump, *PLoS One 9*, e97903.

Lei, H. T., Chou, T. H., Su, C. C., Bolla, J. R., Kumar, N., Radhakrishnan, A., Long, F., Delmar, J. A., Do, S. V., **Rajashankar, K. R.**, Shafer, W. M., and Yu, E. W. (2014) Crystal Structure of the Open State of the *Neisseria gonorrhoeae* MtrE Outer Membrane Channel, *PLoS One 9*, e97475.

Sciara, G., Clarke, O. B., Tomasek, D., Kloss, B., Tabuso, S., Byfield, R., Cohn, R., **Banerjee, S.**, **Rajashankar, K. R.**, Slavkovic, V., Graziano, J. H., Shapiro, L., and Mancia, F. (2014) Structural basis for catalysis in a CDP-alcohol phosphotransferase, *Nat. Commun. 5*, 4068.

Xu, K., Wu, Z., Renier, N., Antipenko, A., Tzvetkova-Robev, D., Xu, Y., Minchenko, M., Nardi-Dei, V., **Rajashankar, K. R.**, Himanen, J., Tessier-Lavigne, M., and Nikolov, D. B. (2014) Structures of netrin-1 bound to two receptors provide insight into its axon guidance mechanism, *Science 344*, 1275-1279.

Demirci, H., **Murphy, F. V. t.**, Murphy, E. L., Connetti, J. L., Dahlberg, A. E., Jogl, G., and Gregory, S. T. (2014) A structural analysis of base substitutions in *Thermus thermophilu*s 16S ribosomal RNA conferring streptomycin resistance, *Antimicrob. Agents Chemother.* 58, 4308-4317.

Su, C. C., Radhakrishnan, A., Kumar, N., Long, F., Bolla, J. R., Lei, H. T., Delmar, J. A., Do, S. V., Chou, T. H., **Rajashankar, K. R.**, Zhang, Q., and Yu, E. W. (2014) Crystal structure of the *Campylobacter jejuni* CmeC outer membrane channel, *Protein Sci. 23*, 954-961.

Radhakrishnan, A., Kumar, N., Wright, C. C., Chou, T. H., Tringides, M. L., Bolla, J. R., Lei, H. T., **Rajashankar, K.**, Su, C. C., Purdy, G. E., and Yu, E. W. (2014) Crystal structure of the transcriptional regulator Rv0678 of *Mycobacterium tuberculosis, J. Biol. Chem. 289*, 16526-16540.

Dow, B. A., **Sukumar, N.**, Matos, J. O., Choi, M., Schulte, A., Tatulian, S. A., and Davidson, V. L. (2014) The sole tryptophan of amicyanin enhances its thermal stability but does not influence the electronic properties of the type 1 copper site, *Arch. Biochem. Biophys.* 550-551, 24-27.

Jain, R., **Rajashankar, K. R.**, Buku, A., Johnson, R. E., Prakash, L., Prakash, S., and Aggarwal, A. K. (2014) Crystal Structure of Yeast DNA Polymerase & Catalytic Domain, *PLoS ONE 9*, e94835.

Lee, K., Lam, K.-H., Kruel, A. M., **Perry, K.**, Rummel, A., and Jin, R. (2014) High-resolution crystal structure of HA33 of botulinum neurotoxin type B progenitor toxin complex, *Biochem. Biophys. Res. Commun. 446*, 568-573.

Poor, C. B., Wegner, S. V., Li, H., Dlouhy, A. C., **Schuermann, J. P.**, Sanishvili, R., Hinshaw, J. R., Riggs-Gelasco, P. J., Outten, C. E., and He, C. (2014) Molecular mechanism and structure of the *Saccharomyces cerevisiae* iron regulator Aft2, *Proc. Nat. Acad. Sci. U.S.A.* 111, 4043-4048.

Rajashankar, K., and Dauter, Z. (2014) Data collection for crystallographic structure determination, *Methods Mol. Biol. 1140*, 211-237.

Kobe, M. J., **Neau, D. B.**, Mitchell, C. E., Bartlett, S. G., and Newcomer, M. E. (2014) The Structure of Human 15-Lipoxygenase-2 with a Substrate Mimic, *J. Biol. Chem. 289*, 8562–8569.

Strunk, R. J., Piemonte, K. M., Petersen, N. M., Koutsioulis, D., Bouriotis, V., **Perry, K.**, and Cole, K. E. (2014) Structure determination of BA0150, a putative polysaccharide deacetylase from *Bacillus anthracis*, *Acta Crystallogr. F 70*, 156-159.

Luo, Z., **Rajashankar, K.**, and Dauter, Z. (2014) Weak data do not make a free lunch, only a cheap meal, *Acta Crystallogr. D 70*, 253-260.

Kumar, N., Radhakrishnan, A., Wright, C. C., Chou, T. H., Lei, H. T., Bolla, J. R., Tringides, M. L., **Rajashankar, K. R.**, Su, C. C., Purdy, G. E., and Yu, E. W. (2014) Crystal Structure of the transcriptional regulator Rv1219c of *Mycobacterium tuberculosis*, *Protein Sci. 23*, 423-432.

Xu, S., Hermanson, D. J., **Banerjee, S.**, Ghebreselasie, K., Clayton, G. M., Garavito, R. M., and Marnett, L. J. (2014) Oxicams Bind in a Novel Mode to the Cyclooxygenase Active Site via a Two-water-mediated H-bonding Network, *J. Biol. Chem.* 289, 6799-6808.

Huang, H., Zeqiraj, E., Dong, B., Jha, B. K., Duffy, N. M., Orlicky, S., Thevakumaran, N., Talukdar, M., Pillon, M. C., Ceccarelli, D. F., Wan, L. C., Juang, Y. C., Mao, D. Y., Gaughan, C., Brinton, M. A., Perelygin, A. A., **Kourinov, I.**, Guarne, A., Silverman, R. H., and Sicheri, F. (2014) Dimeric Structure of Pseudokinase RNase L Bound to 2-5A Reveals a Basis for Interferon-Induced Antiviral Activity, *Mol. Cell 53*, 221-234.

Schormann, N., **Banerjee, S.**, Ricciardi, R., and Chattopadhyay, D. (2013) Structure of the uracil complex of Vaccinia virus uracil DNA glycosylase, *Acta Crystallogr. F*, 1328-1334.

Acknowledgements

NE-CAT is supported by a grant from the National Institute of General Medical Sciences (P41GM103403) and contributions from the following NE-CAT institutional members:

Columbia University
Cornell University
Harvard University
Massachusetts Institute of Technology
Memorial Sloan-Kettering Cancer Center
Rockefeller University
Yale University